Heliyon 10 (2024) e27035

Contents lists available at ScienceDirect

Heliyon

journal homepage: www.cell.com/heliyon

Research article

Exercise preconditioning inhibits doxorubicin-induced cardiotoxicity via YAP/STAT3 signaling

Chuan-Zhi Wang [a,d,e], Heng-Zhi Guo [a], Jing-Zhi Leng [a], Zhi-De Liang [a], Jing-Tai Wang [a], Li-Jie Luo [b], Shi-Qiang Wang [c,**], Yang Yuan [d,*]

[a] School of Physical Education, Qingdao University, Qingdao, China
[b] Jining University and School of Physical Education, Jining, China
[c] Hunan Research Centre in Physical Fitness, Health, and Performance Excellence, Hunan University of Technology, Hunan, China
[d] Cancer Institute of the Affiliated Hospital of Qingdao University and Qingdao Cancer Institute, Qingdao, China
[e] School of Physical Education and Sports Science, South China Normal University, China

ARTICLE INFO

Keywords:
Exercise preconditioning
Doxorubicin
Cardiotoxicity
YAP
STAT3
Cardiac protection

ABSTRACT

Doxorubicin (DOX) possesses strong anti-tumor effects but is limited by its irreversible cardiac toxicity. The relationship between exercise, a known enhancer of cardiovascular health, and DOX-induced cardiotoxicity has been a focus of recent research. Exercise has been suggested to mitigate DOX's cardiac harm by modulating the Yes-associated protein (YAP) and Signal transducer and activator of transcription 3 (STAT3) pathways, which are crucial in regulating cardiac cell functions and responses to damage. This study aimed to assess the protective role of exercise preconditioning against DOX-induced cardiac injury. We used Sprague–Dawley rats, divided into five groups (control, DOX, exercise preconditioning (EP), EP-DOX, and verteporfin + EP + DOX), to investigate the potential mechanisms. Our findings, including echocardiography, histological staining, Western blot, and q-PCR analysis, demonstrated that exercise preconditioning could alleviate DOX-induced cardiac dysfunction and structural damage. Notably, exercise preconditioning enhanced the nuclear localization and co-localization of YAP and STAT3. Our study suggests that exercise preconditioning may counteract DOX-induced cardiotoxicity by activating the YAP/STAT3 pathway, highlighting a potential therapeutic approach for reducing DOX's cardiac side effects.

1. Introduction

Doxorubicin (DOX), a widely used chemotherapy drug, has dramatically improved the survival rates for cancer patients. However, researchers have cautioned that the time- and dose-dependent cardiotoxicity of drugs cannot be overlooked [1]. Previous studies suggested that oxidative stress and inflammation are the leading causes of DOX-induced cardiac injury [2]. Although the pathogenesis of DOX-induced acute cardiotoxicity is somewhat complex, there appears to be a direct link between apoptosis and cardiac injury [3]. Apoptosis is a vital physiological process that plays a crucial role in maintaining homeostasis in organisms [4]. DOX-induced apoptosis in cardiomyocytes significantly to cardiac damage. Consequently, mitigating DOX-mediated apoptosis could present a potential

* Corresponding author. School of Physical Education, Qingdao University, Qingdao, China.
** Corresponding author.
E-mail addresses: suswsq@163.com (S.-Q. Wang), yuanyangofficial@yeah.net (Y. Yuan).

https://doi.org/10.1016/j.heliyon.2024.e27035
Received 14 June 2023; Received in revised form 22 February 2024; Accepted 22 February 2024
Available online 27 February 2024

therapeutic strategy.

Exercise is widely recognized as a non-pharmacological intervention that promotes cardiac function. The classical form of exercise preconditioning (EP) causes repeated transient ischemia and hypoxia in the myocardium through high-intensity intermittent aerobic exercise, triggering an endogenous protective effect that protects the myocardium from subsequent sustained ischemia and hypoxic injury [5]. Recent studies have demonstrated the protective effect of EP against DOX-induced cardiac injury, and the underlying mechanism is hypothesized to be related to regulating apoptotic processes [6].

The pharmacokinetic model of DOX-induced cardiac injury indicated that the peak concentration of DOX in the body occurs between 2 and 12 h after injection [7]. Additionally, the cardioprotective effects produced by exercise training (EP) exhibit a cyclic,

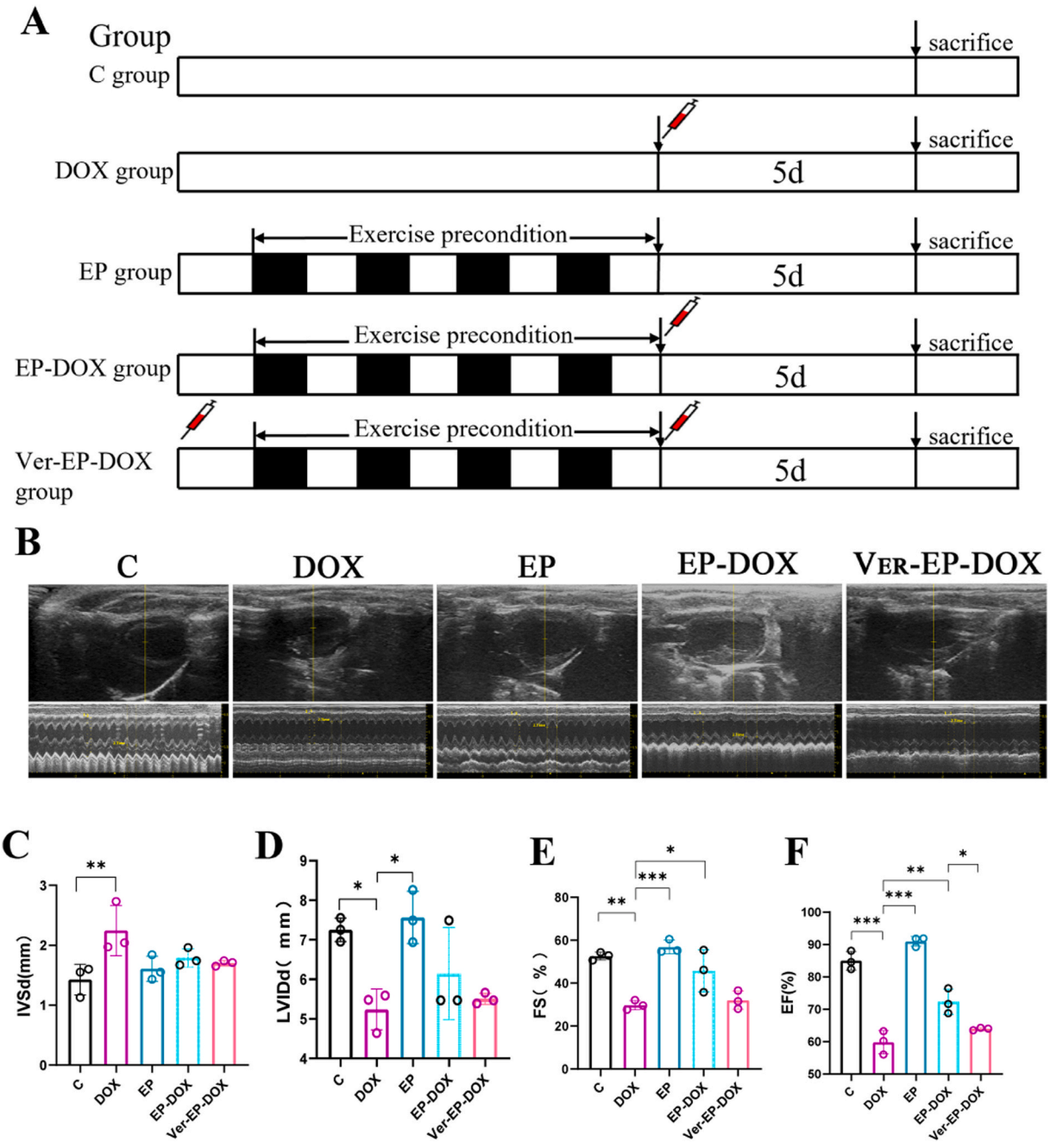

Fig. 1. A, Exercise modeling protocol; B, results of cardiac ultrasound testing in each group; C, interventricular septal thickness (IVSd) statistics; D, LVIDd (left ventricular end-diastolic internal diameter) statistics; E, FS (short-axis shortening rate) statistics; F, EF statistics; "*" indicates P less than 0.05 "**" indicates P less than 0.01, "***" indicates P less than 0.001 the same below.

phase-specific pattern, ranging from immediately post-exercise to 72 h post-exercise, effectively covering the acute injury phase of DOX toxicity [8]. Prior studies have reported the role of exercise interventions in mitigating DOX-induced cardiac toxicity. However, these interventions require a relatively prolonged duration of exercise, which limits their practical applicability and makes it challenging to establish a direct causal relationship between exercise and cardiac protection [9]. Given the immediacy of DOX-induced acute injury and the immediate cardioprotective effects of a single bout of EP, as observed in our previous research findings [10], this study aimed to investigate the underlying protective mechanisms of a single EP intervention.

Yes-associated protein (YAP) is a transcriptional co-activator of the Hippo signaling pathway and has been demonstrated to regulate cell growth, proliferation, differentiation, and migration in developing organs. It is also linked to physiological and pathological processes related to antioxidant capacity and apoptosis regulation [11]. Our previous study demonstrated that YAP exerts cardioprotective effects by stimulating GSH/Bcl-2 interactions. Recently, Tao demonstrated that exercise counteracts DOX-induced heart damage by activating YAP to inhibit Hippo-YAP-mediated apoptosis [12].

Signal transducer and activator of transcription 3 (STAT3) is an essential signaling protein that promotes cardiomyocyte proliferation, angiogenesis, and extracellular matrix homeostasis and reduces the effects of DOX on cardiotoxicity [13,14]. Kunisada et al. observed that DOX treatment significantly reduced cardiac STAT3 gene expression [15]. However, the extent to which exercise treats heart injury through the YAP/STAT3 signaling pathway remains to be determined. In this study, we used verteporfin (VP), a key inhibitor of YAP, to inhibit YAP signaling expression and analyze the mechanisms associated with YAP/STAT3 in EP inhibition of DOX-induced cardiac injury by western blotting, q-PCR, and immunofluorescence double-staining assays.

2. Materials and methods

2.1. Animal study design

For this experiment, 50 19-week-old female Sprague–Dawley rats were purchased from the Spelford Animal Centre (Beijing, China). The rats had an average weight of approximately 300 ± 20 g. They were housed in groups of five rats per cage, maintaining a controlled room environment with a temperature range of 22–24 °C, relative humidity between 40% and 70%, and a daily 12-h light–dark cycle.

Following a five-day acclimatization period, during which the rats were allowed to adapt to their new environment, they underwent a one-week treadmill training regimen. The treadmill exercise consisted of running at a speed of 15 m/min for 15 min without incline (slope 0°). Upon completion of the acclimatization phase, the rats were randomly assigned to five experimental groups: control, doxorubicin (DOX), exercise preconditioning (EP), exercise preconditioning + doxorubicin (EP-DOX), and verteporfin + exercise preconditioning + doxorubicin (Ver-EP-DOX). The EP group engaged in high-intensity intermittent platform running, which entailed running at a speed of 25 m/min (equivalent to 75% of VO_2 max) for 10 min, followed by a 10-min rest period. This cycle was repeated four times, resulting in a total exercise duration of 40 min [16]. The EP-DOX group was administered an intraperitoneal injection of DOX (20 mg/kg) 24 h after EP intervention [17]. The Ver-EP-DOX group received an intraperitoneal injection of DOX (20 mg/kg) 24 h before EP intervention.

The DOX group was administered an intraperitoneal injection of verteporfin (10 mg/kg) 24 h before EP intervention. The specific intervention protocol is illustrated in Fig. 1A. Following the interventions, all rats were anesthetized with sodium pentobarbital (40 mg/kg). An abdominal incision was made along the midline, and a 5 mL blood sample was collected from the inferior vena cava. An infusion needle was then inserted into the left ventricle through the apex of the heart for anticoagulation with sodium heparin and for perfusion with 0.85% saline. Subsequently, the inferior vena cava was incised to allow for drainage [18]. Once the liver was free of blood, the heart was swiftly excised, and tissue samples from the left ventricular wall near the apex were collected. These tissue fragments were rapidly frozen in liquid nitrogen and stored at −80 °C for further analysis. For histological analysis, post-saline perfusion was supplemented with 4% paraformaldehyde, and excised hearts were fixed in 4% paraformaldehyde for 24-h period. The Qingdao University's Institutional Ethics Committee (QDU-HEC-2022058) and the National Institutes of Health's guidelines on the Care and Use of Laboratory Animals sanctioned the entirety of the animal experimental procedures undertaken in this study. We ensured the implementation of all possible measures to alleviate any distress or discomfort experienced by the rats.

2.2. Animal sampling and index testing

2.2.1. Echocardiography

Cardiac ultrasound tests were performed to measure cardiac function indicators in each group of rats. Rats were anesthetized by placing them in an anesthesia machine containing 2% isoflurane, an inhalation anesthesia gas for animals (Rivard R5835, Vaporizer for isoflurane, China; Rivard R546W, Gas Recycler, China; Rivard R510-29, Anesthetic Air Pump, China). After anesthesia, the rats' chest hair was shaved to expose the skin of the heart area. The rats were fixed on a cardiopulmonary function test and electrocardiogram (ECG) testing platform, coated with ultrasound conduction gel to optimize visibility, and tested for cardiac function using a high-resolution echocardiography imaging system (Feinuo V6, China).

2.2.2. Blood sample and myocardial tissue sample collection and processing

After the rat heart ultrasound test was completed, the rats were anesthetized by intraperitoneal injection of sodium pentobarbital (40 mg/kg body weight) and fixed in the supine position on a dissecting table after anesthesia. The abdominal cavity was opened, and 5 mL of blood was extracted from the abdominal aorta, left to stand for 30 min at room temperature, then centrifuged at 4000 g/min for

10 min in a low-temperature centrifuge to extract the serum, and stored in a refrigerator at −20 °C. Five rats in each group were randomly selected for perfusion fixation: a perfusion needle was inserted into the apical part of the heart, and 2 mL of 1% heparin was injected, followed by a rapid infusion of 230–250 mL of 0.9% physiological saline. After the blood was basically colorless, the heart was removed and washed with phosphate-buffered saline (PBS) to clean the residual blood and then fixed in 4% paraformaldehyde at room temperature for 24 h. Paraffin was routinely embedded, and adjacent sections were prepared for subsequent histological staining, where the thickness of each section was 5 μm. The remaining five rats in each group were anesthetized, the thoracic cavity was opened, and the hearts were removed, stored at −80 °C, and used for immunoblotting experiments.

2.2.3. Myocardial injury marker testing

Rat blood samples were kept at room temperature for 30 min until the serum precipitated and then centrifuged at 3500 g/min for 10 min in a low-temperature centrifuge for serum extraction. Cardiac troponin I (c Tn I) was measured using a cardiac troponin I kit (Solarbio, China). Lactate dehydrogenase (LDH) was measured using a lactate dehydrogenase kit (Solarbio, China) according to the manufacturer's instructions specified in the kit. Malondialdehyde (MDA) was measured in the myocardial homogenate supernatant using a malondialdehyde assay kit (Solarbio, China).

2.2.4. Myocardial histopathology testing

Rat hearts were fixed in paraformaldehyde at room temperature for 24 h and then embedded in paraffin. Heart sections were stained with hematoxylin and eosin (H&E) stain to analyze cardiac morphology and Masson stain to analyze myocardial fibrosis, and all sections were cut longitudinally [13].

2.2.5. Immunohistochemical inflammatory marker IL-1β staining of myocardial tissue

The sections were incubated in 3% H_2O_2 for 10 min at room temperature, rinsed in PBS, blocked in goat serum, and incubated overnight at 4 °C with IL-1β antibody. The sections were then incubated for 15 min at 37 °C with secondary antibodies, washed with PBS, and stained with 0.05% diaminobenzidine for 1 min and hematoxylin for 5 min. Finally, they were dehydrated, permeabilized, and sealed with neutral gum. Cells positive for IL-1β staining were observed under a microscope (Nikon AIR HD25, Japan), and the area of the positive region was calculated using ImageJ software for image processing.

2.2.6. Western blotting

The expression of apoptosis-related proteins in rat myocardial tissue was analyzed using protein immunoblotting (western blotting). Total protein was extracted from rat myocardial tissue, and the protein concentration was adjusted by BCA protein quantification. After SDS gel electrophoresis and membrane transfer, primary antibodies (Cytc, Bcl-2, BAX, caspase-3, YAP, P-YAP, STAT3, P-STAT3, JAK2, MST1, LATS1, and GAPDH) were incubated for 1 h in 5% skimmed milk. Antibody dilutions were all 1:1000. Antibodies were purchased from Seville Biotechnology, Ltd. The primary antibody was a rabbit monoclonal antibody, which was incubated overnight at 4 °C with HRP-labeled secondary antibody for 1 h. ECL luminescence, a gel imaging system, was used to capture images, and the expression level of each protein was estimated using ImageJ. The gray values of the specific bands in the images were scanned and measured using ImageJ (NIH, Bethesda, MD, USA).

2.2.7. Detection of YAP mRNA/STAT3mRNA expression via qRT-PCR

TRIzol method was used to extract mRNA from the heart tissues of rats in each group. The reverse transcription reaction conditions were set as follows: 25 °C for 10 min, 42 °C for 50 min, and 85 °C for 5 min. The fluorescent quantitative PCR amplification conditions were set as follows: 94 °C for 4 min, 94 °C for 20 s, 60 °C for 30 s, 72 °C for 30 s, and 35 cycles, and the signal was detected at 72 °C. The relative expression of YAP mRNA, STAT3mRNA, and Bcl-2mRNA was calculated using the $2^{-\Delta\Delta Ct}$ method. The target gene sequences are listed in Table 1. The introduction sequence of this article was synthesized and purified by the Shanghai Bioengineering Company based on primer design principles and computer gene nucleotide sequence data.

2.2.8. Co-localization of YAP and STAT3 detected via immunofluorescence double-labeling

After dewaxing in water, the sections were washed with PBS thrice, digested with a pepsin complex at room temperature, and then immersed again in PBS. Goat serum was used as the blocking reagent. For double-labeled immunofluorescence staining, the antibodies were mixed, added to the tissue sections, and then incubated for 24 h at 4 °C. The same procedure was adopted for the mixture of the anti-YAP rabbit antibody (anti-rat, 1:500, Cell Signaling, MA, USA) and anti-STAT3 mouse antibody (anti-rat, 1:200, Santa Cruz, CA, USA) added to different tissue slices. PBS was used as the negative control instead of the primary antibody. A fluorescein-labeled secondary antibody mixture of FITC (anti-rabbit, 1:200, Biyuntian Biotech, Jiangsu, China) and CY3 (anti-mouse, 1:200, Biyuntian

Table 1
Target gene sequence.

Gene	Forward (5 , -3 ,)	Reverse (5 , -3 ,)
STAT3	TAT CTT GGC CCT TTG GAA TG	GTG GGG ATA CCA GGA TGT TG
YAP1	CCC CAG ACG CTG ATG AAC TC	GGG TCC AGC CAG GAT GTG
Bcl-2	CTG GTG GAC AAC ATC GCT CT	CAT CCC AGC CTC CGT TAT CC
GAPDH	TAT CGG ACG CCT GGT TAC	GTC TTC TGA GTG GCA GTG AT

Biotech, Jiangsu, China) was used for detection. The slides were incubated in the dark at 37 °C, and the nuclei were stained with DAPI. Image analysis was performed using IMARIS X64 9.0.1 software, and red and green fluorescent pixel point distributions were estimated using four-quadrant scatter plots. Further data included the fluorescence intensity of positive regions and the percentage of co-localization coefficients (Manders' co-localization coefficients, MCC).

2.2.9. Data statistics and analysis

Data were analyzed using SPSS 25.0 (IBM, Chicago, IL, USA). One-way ANOVA was used to determine significant group differences

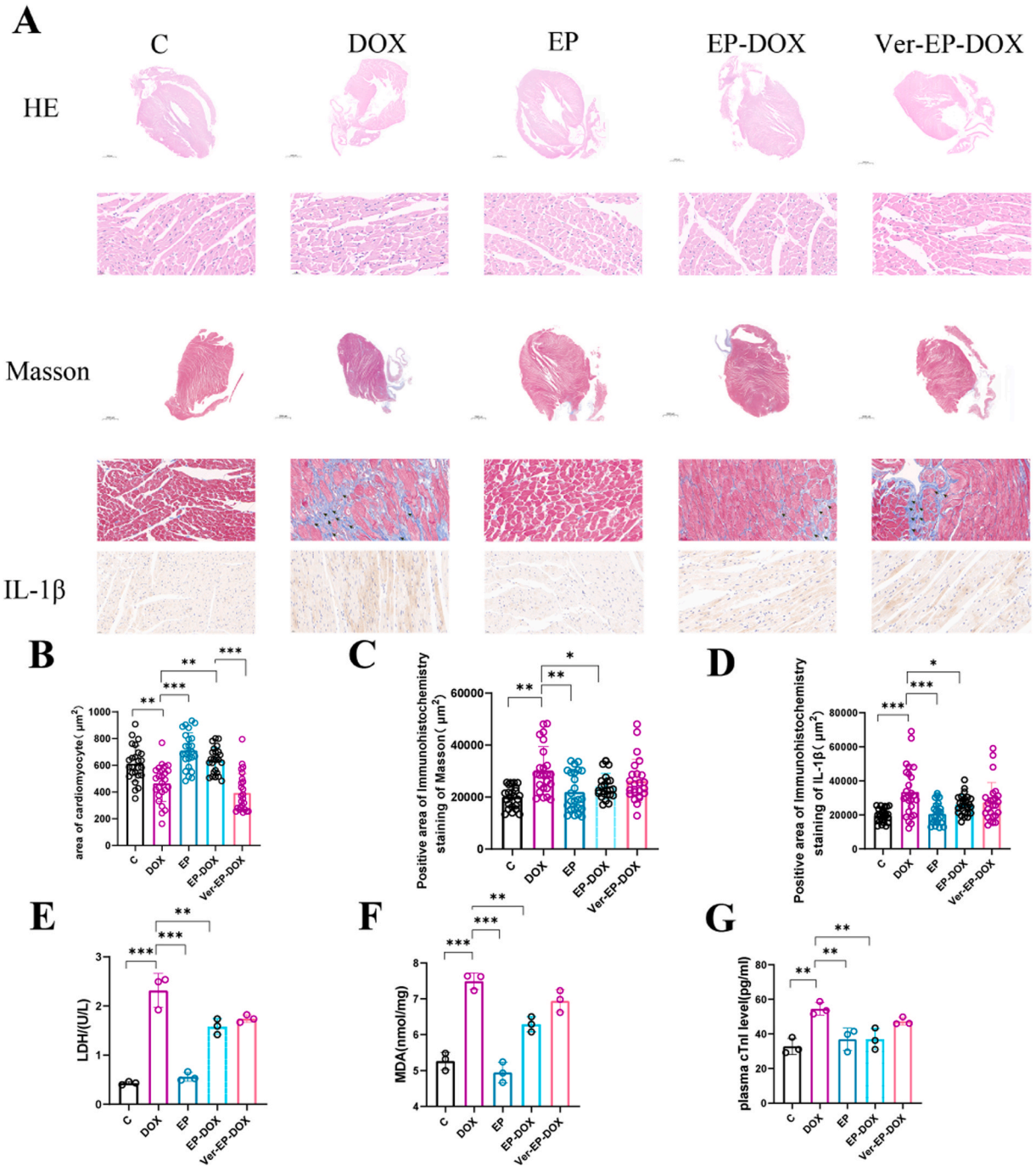

Fig. 2. A, Pathological staining statistics of each group (section thickness was 5 μm); B, H&E staining quantitative analysis of the cardiomyocyte area; C, Masson staining quantitative statistics of the positive area; IL-1β staining quantitative statistics of the positive area.

based on pairwise comparisons and to determine the major effects. Post-hoc contrasts were analyzed using the Student–Newman–Keuls (SNK) test. The results are expressed as the mean ± SD, and a *P*-value <0.05 was regarded as statistically significant.

3. Results

3.1. EP improves DOX-induced cardiac dysfunction

To examine the impact of EP on DOX-induced cardiotoxicity, we created a rat model of DOX-induced cardiotoxicity. Echocardiography was performed in the control, DOX, EP, and EP-DOX groups to assess cardiac function. At the end of the experiment, a trend toward increased LVIDd and IVSd was observed in the DOX-treated rats. DOX treatment significantly reduced LV systolic function, including EF and FS, compared with that in the control group (Fig. 1E and F). LV systolic dysfunction was alleviated in rats treated with EP compared with that in the DOX group (Fig. 1C–F). The above findings suggest that EP exerted beneficial effects on DOX-induced cardiac dysfunction, and the cardioprotective effects of EP were diminished after the blockade of YAP signaling.

3.2. EP ameliorates DOX-induced histomorphological and pathological changes in the myocardium

To investigate the protective effects of EP against DOX-induced myocardial changes, we conducted H&E staining (Fig. 2A and B). The hearts of control mice exhibited a typical structure in H&E staining, whereas the DOX group displayed several changes in the myocardium compared with the control group. These changes include necrosis, intracellular edema, myogenic fiber disorganization, and myocardial fiber ripple degeneration. Notably, these pathological phenomena were effectively mitigated in the EP-DOX group compared with those in the DOX group. Additionally, we assessed the protective effect of EP on DOX-induced myocardial fibrosis using Masson's staining, with the fibrotic area depicted in blue in the figure. We quantified the collagen fiber area using ImageJ, and the results indicated a significantly higher myocardial fibrotic area in the DOX group than in the control group ($P < 0.05$). Conversely, myocardial fibrosis in the EP-DOX group was significantly lower ($P < 0.05$) than that in the DOX group (Fig. 2A–C). To explore the effect of DOX on cardiomyocyte inflammation, we employed IL-1β staining. The results revealed a significantly greater inflamed area ($P < 0.05$) in the DOX group than that in the control group (Fig. 2D). In contrast, the inflamed area was notably reduced ($P < 0.05$) in the EP-DOX group compared with that in the DOX group.

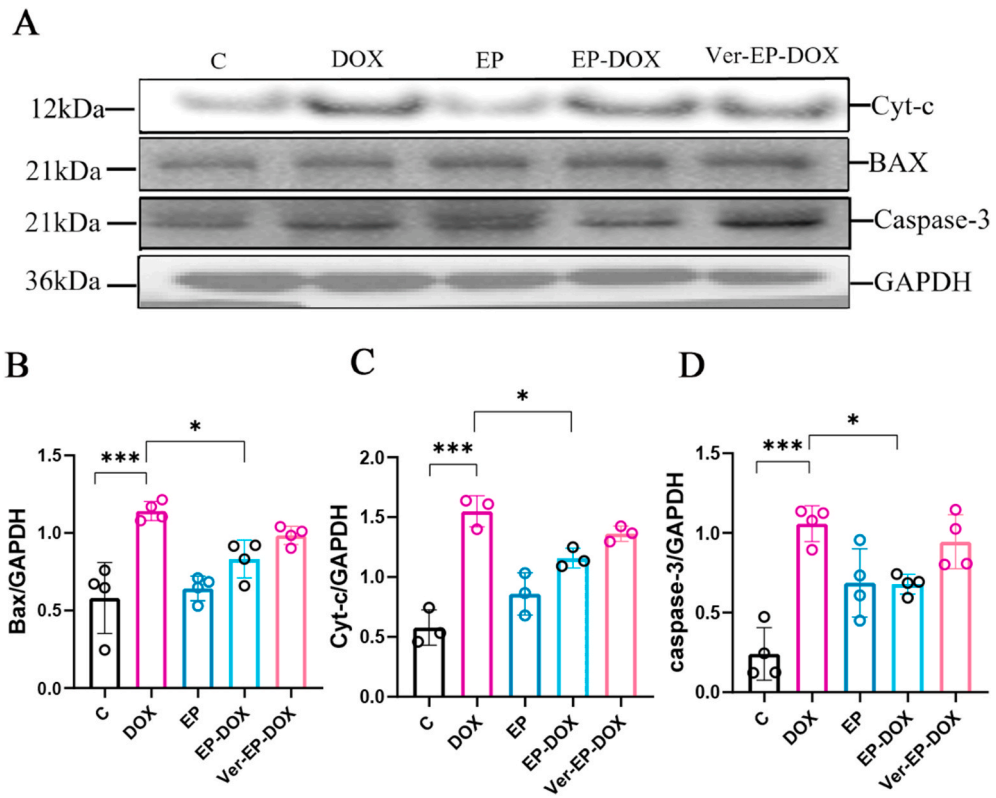

Fig. 3. A, Statistical results of apoptosis-related proteins in each group by movement; B, statistical results of the gray value of BAX protein compared with that of internal reference protein; C, Gray value of Cyt-c compared with that of the internal reference protein; D, statistical results of the gray value of caspase-3 compared with that of the internal reference protein.

We also analyzed the cardiac injury markers MDA, LDH, and cTnI and found that DOX significantly increased the expression of MDA, LDH, and cTnI compared with the control group (Fig. 2E–G). EP treatment significantly reduced the DOX-induced increase in these indices compared with the DOX group (Fig. 2E–G). In conclusion, EP ameliorates the effects of DOX on myocardial fibrosis, inflammation, and cardiac injury.

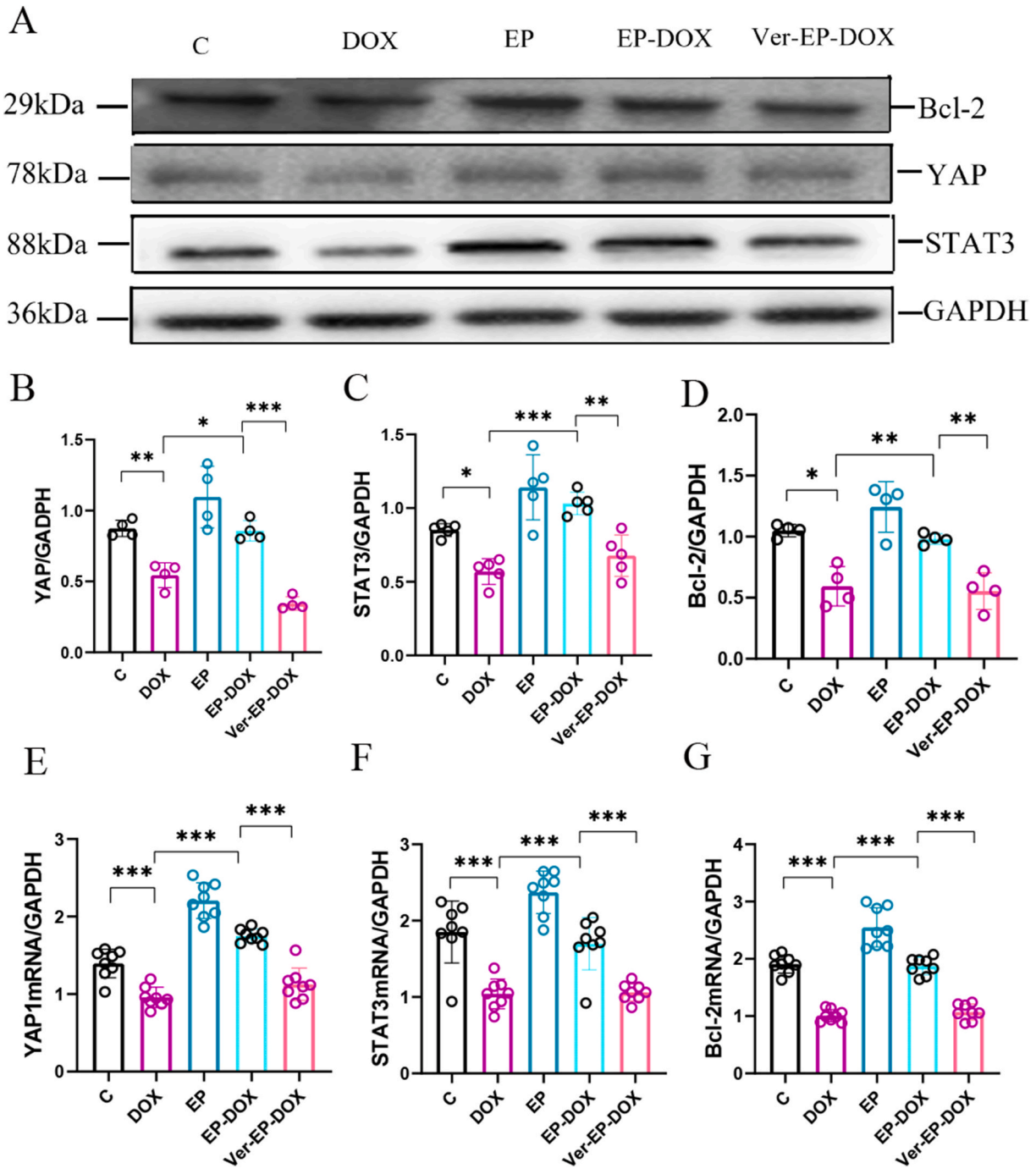

Fig. 4. A, Bands of Bcl-2, YAP1, STAT3, and the internal reference GAPDH for each group. B, statistical results of YAP1 protein gray value over the internal reference protein; C, statistical results of STAT3 protein gray value over the internal reference protein; D, statistical results of Bcl-2 protein gray value over the internal reference protein; E, statistical results of YAP1 gene over the internal reference gene; F, statistical results of STAT3 gene over the statistical results of the inner reference gene; Bcl-2 gene over the inner reference gene.

3.3. EP regulates apoptosis protein expression to resist DOX-induced apoptosis in cardiomyocytes

Our histological examination demonstrated the effects of DOX on myocardial fibrosis, inflammation, and histological damage. To further examine the impact of DOX on myocardial apoptosis, we measured the expression of apoptosis-related proteins, including BAX, caspase-3, and Bcl-2, as well as the mitochondrial damage protein Cytc, in myocardial tissue by protein blotting. We compared the DOX group with the control group. The expressions of BAX, Cytc, and caspase-3 were significantly increased ($P < 0.05$) in the DOX group than in the control group (Fig. 3A–C). EP treatment significantly reduced the expression of apoptotic proteins ($P < 0.05$; Fig. 3B–D). Conversely, Bcl-2, an anti-apoptotic protein, was significantly downregulated in the DOX group. However, its expression was restored in rats treated with EP (Fig. 4D). In conclusion, our results suggest that EP protected against DOX-induced apoptosis in cardiac myocytes.

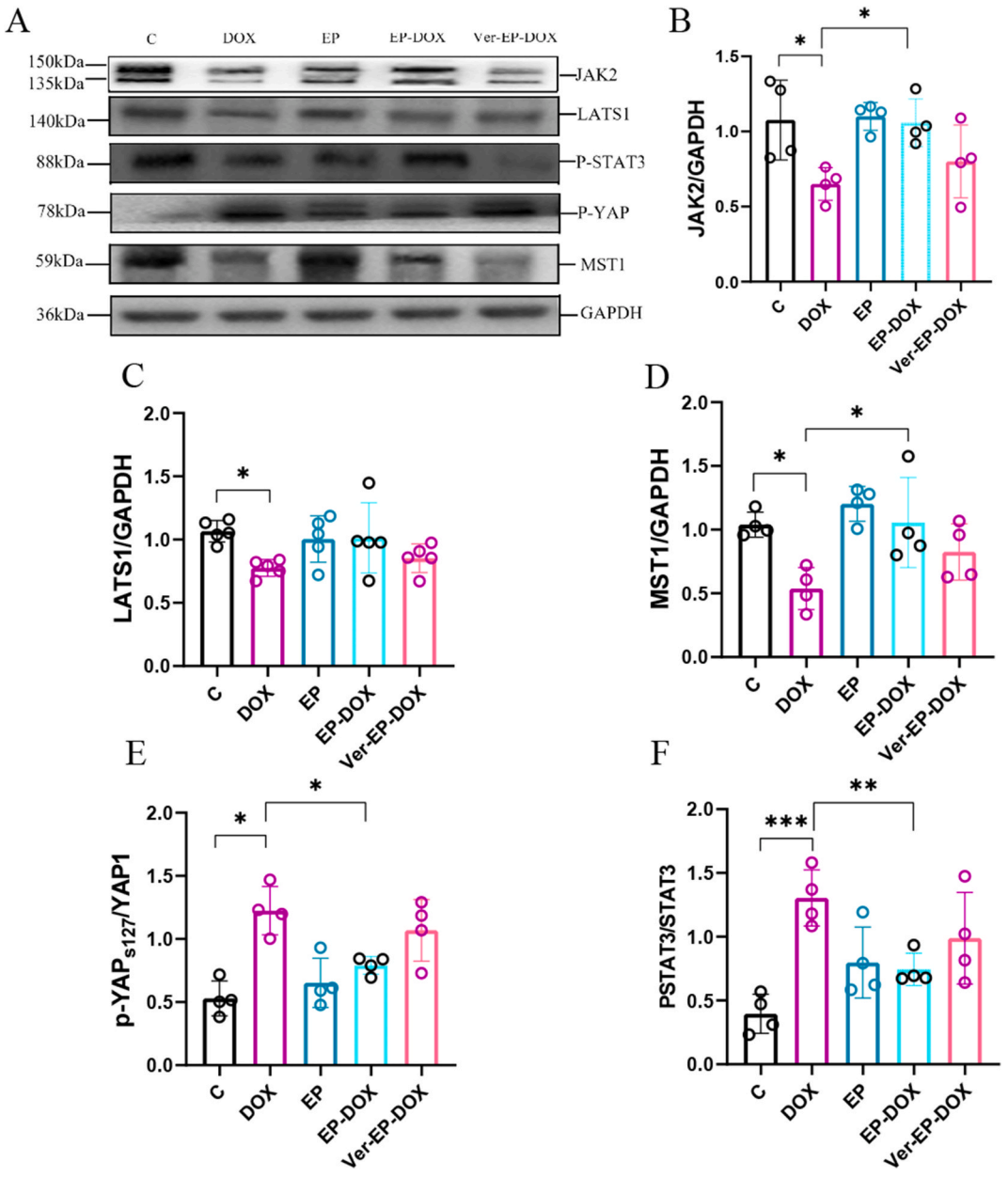

Fig. 5. A, Expression of YAP1/STAT3-related pathway proteins by EP; B, statistical results of the effects of EP on JAK2 in DOX-injected rats; C, statistical results of the effects of EP on LATS1 protein in DOX-injected rats; D, statistical results of the effects of EP on MST1 protein in DOX-injected rats; E, statistical results of the effects of EP on the level of phosphorylation of YAP1 in DOX-injected rats (P-YAPs 127 inhibitory site); F, statistical results of the effects of EP on the level of STAT3 phosphorylation in DOX-injected rats.

3.4. EP attenuates DOX-induced apoptosis by promoting STAT3 expression

In our study, we observed that compared with the control group, the expressions of STAT3 mRNA and STAT3 protein were suppressed in the DOX group (Fig. 4C and F). Concurrently, the expression of the anti-apoptotic protein, Bcl-2, was downregulated (Fig. 4C and F). Notably, when comparing the DOX group with the EP-DOX group, we observed a restoration of STAT3 expression ($P < 0.05$), accompanied by an increase in Bcl-2 expression (Fig. 4D and G). Furthermore, our investigation revealed a decrease in YAP expression in the DOX group than the control group, indicating the activation of Hippo-YAP signaling. In conjunction with the results of Bcl-2 immunoblotting, we hypothesized the occurrence of myocardial apoptosis. Compared with the control group, EP significantly enhanced the expressions of YAP, Bcl-2, and STAT3 genes and proteins. Importantly, it is worth noting that in the VER-EP-DOX group, compared with the EP-DOX group, varying degrees of decline were observed in the expressions of YAP, STAT3, and Bcl-2. This suggests that the protective effect of EP against DOX-induced injury was attenuated after blocking YAP signal (Fig. 4A–E).

3.5. EP inhibits DOX injury by mediating the activation of YAP/STAT3-related pathways

To further investigate the protective effects of EP on the heart through the YAP/STAT3-related pathway, we performed immunoblotting to assess the expressions of JAK2, LATS1, P-STAT3, P-YAP, and MST1 proteins in rat myocardium. The grayscale values of each protein were quantified using ImageJ. Our findings revealed that compared with the control group, DOX significantly inhibited the phosphorylation levels of JAK2, LATS1, MST1, and STAT3 while promoting the phosphorylation level of YAP ($P < 0.05$; Fig. 5A–F).

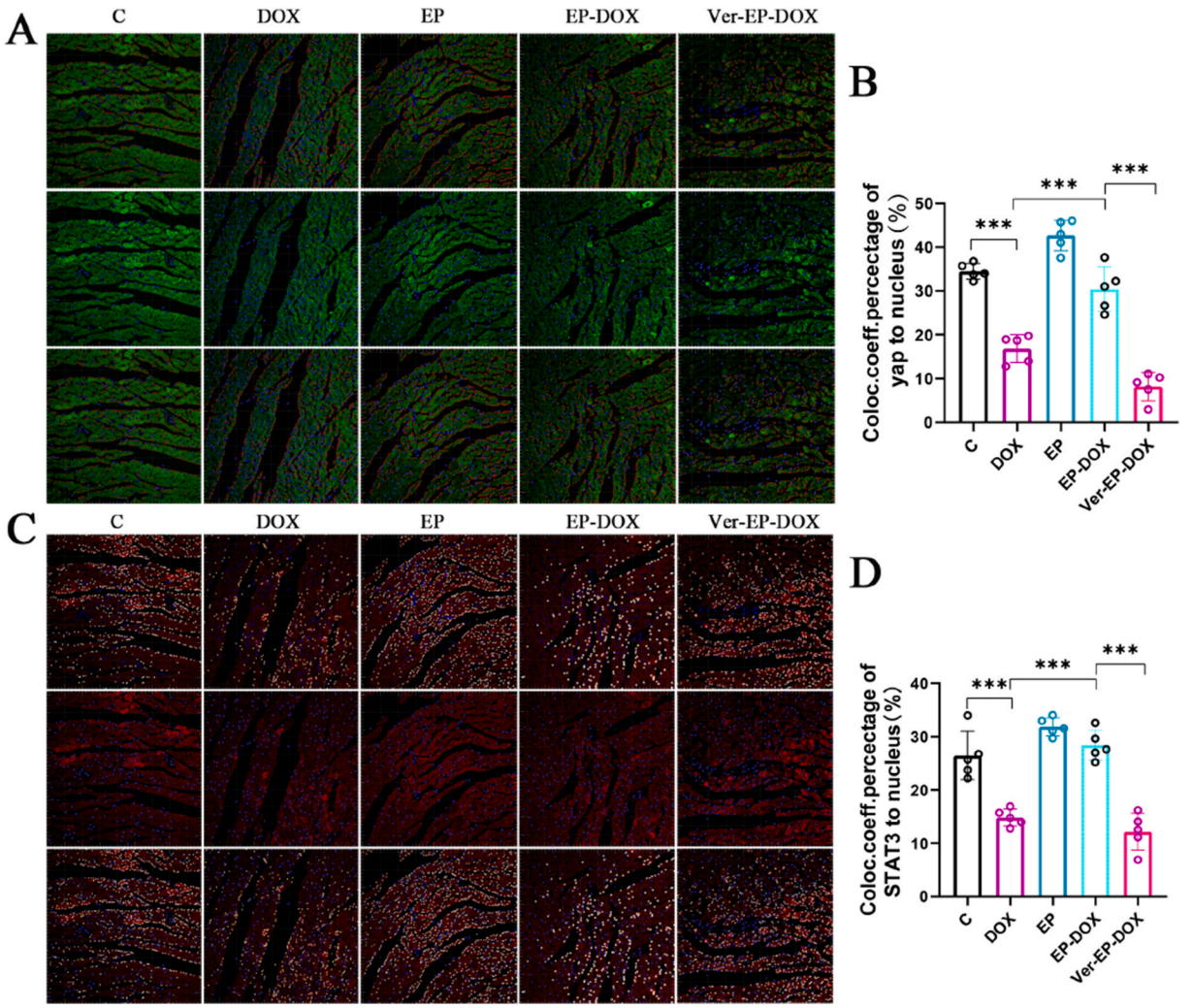

Fig. 6. A, Fluorescence staining images of YAP1 in each group (blue is DAPI-stained nuclei; green is the positive area of YAP1 antibody, quantified by red spheres, section thickness is 5 μm); B, statistical results of the effect of EP on the nuclear localization of YAP1 in DOX-injected rats; C, fluorescence staining images of STAT3 in each group (blue is the nuclei stained by DAPI; red is the positive area of STAT3 antibody, quantified by white spheres, section thickness is 5 μm); D, statistical results of the effect of EP on the nuclear localization of STAT3 in DOX-injected rats.

Compared with the control group, EP significantly upregulated the expression of MST1 ($P < 0.05$). Furthermore, compared with the DOX group, the EP-DOX group exhibited significantly higher expression of P-YAP ($P < 0.05$; Fig. 5F). In contrast, the VP-EP-DOX group exhibited significantly lower expressions of P-STAT3 and MST1 ($P < 0.05$) than the EP-DOX group, without significant change in JAK2 expression, whereas P-YAP expression was significantly higher (Fig. 5A–F).

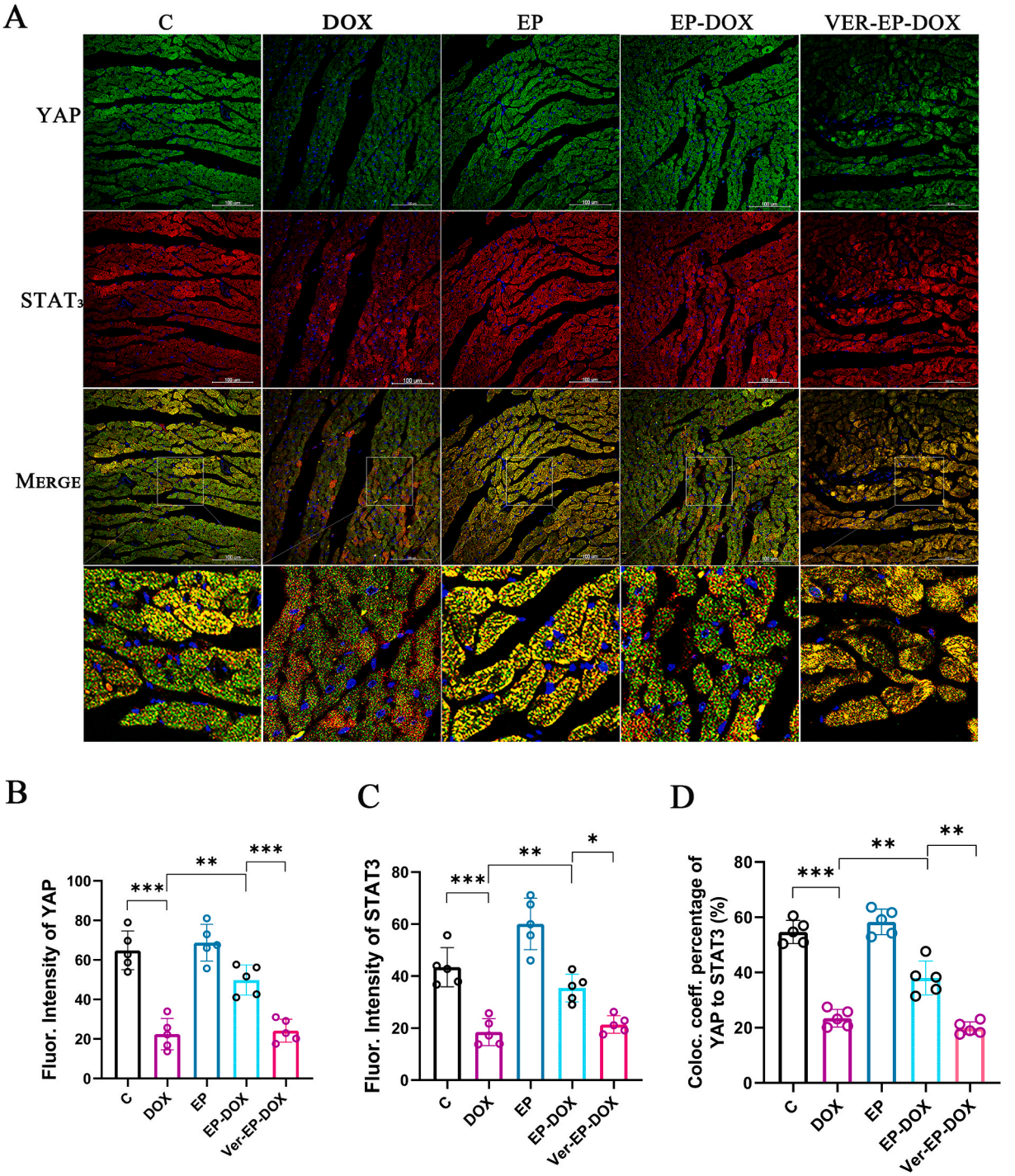

Fig. 7. A, YAP/STAT3 immunofluorescence double-labeled images of each group (the green area is the YAP-positive area, blue is the nucleus, red is the STAT3-positive area, and co-localized area of the two is yellow); B, fluorescence intensity statistics of YAP; C, fluorescence intensity statistics of STAT3; D, co-localization degree statistics of YAP and STAT3.

3.6. EP promotes YAP/STAT3 co-localization

Our experimental results indicate that DOX inhibited the nuclear localization of YAP (Fig. 6A、6C). YAP localization is marked by green fluorescence, whereas blue fluorescence represents the cell nuclei. Our analysis, conducted using IMARIS X64 9.0.1, revealed a significantly reduced nuclear localization of YAP in the DOX group compared with the control group ($P < 0.05$). In contrast, EP markedly promoted the nuclear localization of YAP compared with the control group ($P < 0.05$). Furthermore, the EP-DOX group displayed a higher degree of nuclear localization than the DOX group ($P < 0.05$; Fig. 6B). The verteporfin inhibitor group significantly impeded the nuclear localization of YAP. In Fig. 6, red fluorescence highlights the nuclear localization of STAT3, whereas blue fluorescence represents the cell nuclei. The data displayed that STAT3 nuclear localization in the DOX group was significantly lower than that in the control group ($P < 0.05$). Conversely, the EP-DOX group exhibited a significantly higher level of STAT3 nuclear localization than the DOX group (Fig. 6D), without significant change observed in STAT3 nuclear localization in the verteporfin inhibitor group.

We expanded our investigation into the role of YAP/STAT3 in the cardioprotective effects of EP by using immunofluorescence double-labeling to detect YAP and STAT3 co-localization. The co-localization findings (400 × magnification, bar = 100 μm) revealed that in the control group, YAP, indicated by green immunofluorescence, was evenly distributed in the cardiomyocytes, with blue staining marking the nuclei. STAT3 was labeled with red immunofluorescence within the same group, resulting in granular aggregates within cells with blue-stained nuclei. The merged images of the control group depicted yellow staining, indicating YAP and STAT3 co-localization. In contrast to the control group, the DOX group displayed dispersed green YAP fluorescence and reduced YAP and STAT3 co-localization. After EP intervention, the fluorescence intensity and co-localization of YAP and STAT3 in the EP group were significantly higher than in the DOX group (Fig. 7A–D). Verteporfin-induced YAP signal blockage significantly suppressed YAP/STAT3 co-localization and fluorescence intensity, similar to the DOX group. Our findings suggest that the cardioprotective effects of EP may be linked to the YAP/STAT3 pathway.

4. Discussion

This study demonstrated that performing high-intensity intermittent exercise as a preconditioning measure 24 h prior to DOX administration can effectively attenuate acute cardiac injury following DOX injection. The mechanism may involve the effective inhibition of DOX-induced apoptosis by EP. Additionally, DOX treatment reduced the expressions of YAP and STAT3, as well as the degree of co-localization between YAP and STAT3. These findings suggest that EP may exert a protective effect by inhibiting DOX-induced cardiomyocyte apoptosis through the YAP/STAT3 pathway.

In the clinical field, many strategies have been implemented to address DOX-induced cardiotoxicity, including classical medicine and novel non-coding RNAs [19]. However, there is still a lack of adequate protective agents. Inhibiting DOX cardiotoxicity is of clinical value. The beneficial effects of exercise on cardiovascular health have been widely demonstrated over the years [20]. Although the effectiveness of aerobic exercise for DOX-induced cardiotoxicity has been established, it should be noted that in chemotherapy patients, low clinical compliance with long exercise cycles may be expected. Conversely, the risks of prolonged exercise, such as promoting the production of free radicals, including reactive oxygen species, which are detrimental to treating DOX injuries, should not be overlooked [21]. Consequently, it is worth exploring methods to maximize the cardioprotective effects of exercise in the shortest amount of time. The EP model in this study follows the concept proposed by Domenech et al. which suggests that repeated short bursts of high-intensity intermittent aerobic exercise can produce an endogenous cardioprotective effect similar to ischemic preconditioning (IP), resulting in myocardial protection against subsequent sustained ischemic–hypoxic injury [22]. Pharmacokinetic modeling of DOX cardiac injury suggests that the peak concentration of DOX in the body occurs between 2 and 12 h after injection [7]. The cardioprotective effects of EP are better equipped to handle the acute damaging effects of DOX in vivo [8,9]. Consequently, a single EP demonstrated sound cardioprotective effects in this study.

Masson's staining and quantitative analysis of IL-1β revealed significant fibrosis and inflammatory changes in the myocardium induced by DOX. Inflammatory cells prominently infiltrated the matrix, and myocardial fibers underwent dissolution and rupture. Simultaneously, cardiac ultrasound findings suggested that DOX-induced myocardial damage could lead to further changes in the cardiac structure, enlargement of the ventricular chambers, and a decrease in cardiac pumping function (LVEF), an actual cause of DOX-induced heart failure. Previous studies have displayed that acute stress can rupture myocyte membranes, break myogenic fibers, and leak LDH and cTnI from inside the cells into the blood, dramatically increasing plasma cTnI and LDH levels [23]. In this study, we found that DOX increased the levels of MDA, LDH, and cTnI, markers of oxidative stress injury in cardiomyocytes, and leaked into the blood, resulting in increased plasma cTnI and LDH levels. In this study, cTnI levels in the EP-DOX group were close to those in the control group, which we hypothesize is related to the return of cardiac injury markers to baseline levels five days after the intervention in hearts protected from acute DOX injury by EP. Previous studies have revealed that exercise-induced cTnI elevations gradually return to baseline levels within 24 h [24].

Furthermore, DOX causes myocardial oxidative stress damage, and cardiomyocytes with abundant mitochondria lack antioxidant enzyme properties and are more susceptible to DOX attacks [25]. Moreover, increased ROS production leads to the activation of apoptosis regulators, such as the Bax protein tested in this study, which facilitates the release of Cytc from the mitochondrial membrane [26]. This process leads to a cascade of events in the caspase-3/caspase-9 apoptosis pathway, ultimately leading to cardiomyocyte apoptosis [27]. Bcl-2 is an essential anti-apoptotic gene, whereas Bax promotes apoptosis. On the one hand, the Bax protein forms a heterodimer with Bcl-2 and reduces its expression; on the other hand, it displays a pro-apoptotic effect, and overexpression leads to cell death [28]. In this study, DOX was found to induce a decrease in Bcl-2 expression and an increase in Bax and

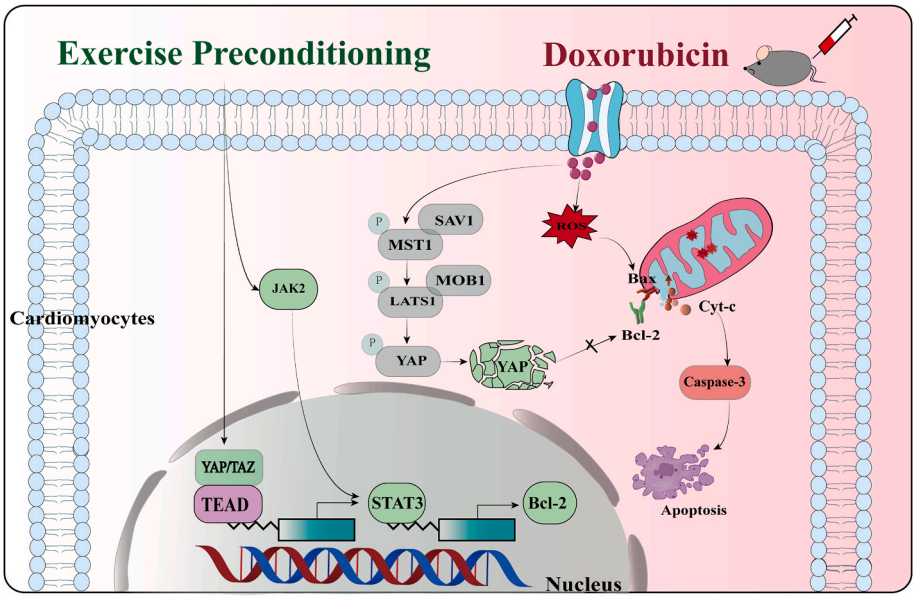

Fig. 8. Possible mechanisms of exercise pre-adaptation to inhibit DOX-induced cardiac injury through the YAP and STAT3 pathways.

cytoplasmic Cytc expressions, suggesting that DOX may be involved in apoptosis development and progression by inhibiting Bcl-2 and promoting Bax expression, thereby inducing the formation of cardiomyopathy (Fig. 8).

The primary pathophysiology of DOX-mediated cardiotoxicity is ascribed to excessive oxidative stress, leading to cell death [29]. To uncover downstream mechanisms, we found that YAP/STAT3 signaling may be crucial in EP-induced cardioprotection. YAP plays a crucial role in cardiac development, myocardial infarction (MI), and fibrosis. In chronic MI, cardiomyocyte-specific deletion of YAP exacerbates MI-induced cardiomyocyte apoptosis and cardiac dysfunction [30]. Exercise mitigates the risk of DOX-induced cardiac injury by blocking the activation of the HIPPO-YAP pathway [12]. In the current study, we found that the downregulation of MST1 and LATS1 protein expression after DOX treatment led to the activation of Hippo-YAP signaling, resulting in the phosphorylation of MST1/2, LATS1, and YAP, leading to YAP degradation. This resulted in the inability of YAP to regulate the Bcl-2 gene, a decrease in intracellular Bcl-2, and subsequent apoptosis of cardiomyocytes (Fig. 8). STAT3 has been reported to be vital in reducing oxidative stress in cardiac pathological conditions [31]. STAT3 deficiency leads to severe fibrosis and enhances cardiomyocyte apoptosis after ischemia–reperfusion. Increased levels of STAT3 phosphorylation may be a significant indicator of DOX-induced heart failure [32]. Previous studies have demonstrated that exercise increases cardiac JAK2 and STAT3 expression, reduces caspase-3 expression, and slows down cardiomyocyte apoptosis. As a crucial transcription factor in cell proliferation and survival signaling, STAT3 is critical in protecting against stress-induced cardiac injury. Previous studies have indicated that DOX inhibits STAT3 expression and further suppresses Bcl-2 nuclear gene expression, resulting in reduced intracellular Bcl-2 expression and increased Bax levels, leading to cytochrome C release and activation of the caspase-3 apoptosis pathway (Fig. 8) [31]. In this study, we discovered that DOX inhibited STAT3 expression and simultaneously suppressed Bcl-2 expression. EP reversed the adverse effects of DOX. We noted that EP promoted STAT3 phosphorylation levels and JAK2 signaling and speculated that EP, as a specific form of IP, may be involved in anti-DOX cardiac injury via JAK2/STAT3. Furthermore, previous studies have found that YAP and TAZ interact directly with JUNB and STAT3 through the WW structural domain necessary for transformation and that they stimulate transcriptional activation of AP-1 proteins [33]. VP is a YAP inhibitor that induces YAP phosphorylation and cleavage of caspase-3 and PARP [34]. The degree of YAP/STAT3 co-localization was significantly reduced with VP, while the level of P-STAT3 increased. As an inhibitor of YAP, we validated its protective effects, with a previous study confirming that in vivo injection of verteporfin in mice with permanent cardiac ischemia significantly reduced fibrosis and morphological remodeling but did not improve cardiac performance [35]. We also tried to ascertain whether verteporfin alone could cause an improvement in cardiac function, but the Masson's assay suggested that verteporfin attenuates cardiac fibrosis (Supplementary Figs. 1 and 2). We also hypothesized that such a single injection would be insufficient to affect acute cardiac injury. In conclusion, we suspect that VP interferes with YAP/STAT3 transcriptional signaling. Based on the results of q-PCR and immunofluorescence experiments, we propose that EP regulates DOX-induced cardiac injury by regulating YAP/STAT3 signaling in the nucleus.

5. Conclusions

Based on our experimental results, we conclude that EP markedly reduces DOX-induced cardiotoxicity, improves heart function, and suppresses myocardial inflammation and fibrosis, which are closely linked to cellular apoptosis. According to our findings, EP enhances the expression and co-localization of YAP/STAT3, leading to upregulation of Bcl-2 expression, facilitation of Bax–Bcl-2 interaction, inhibition of cytochrome C release from the mitochondrial membrane, and subsequent suppression of the caspase-3

pathway cascade involved in apoptosis induction. We propose that YAP and STAT3 pathways can serve as significant targets in EP treatment of DOX-induced cardiotoxicity.

Funding statement

This work was supported by the National Natural Science Foundation of China (No. 32000830) and special funding from the China Postdoctoral Fund Station (No. 2021T140356). We thank Home for Researchers editorial team (www.home-for-researchers.com) for language editing service.

Data availability statement

The datasets used and/or analyzed in this study are available upon reasonable request from the corresponding author.

CRediT authorship contribution statement

Chuan-Zhi Wang: Writing – review & editing, Writing – original draft. **Heng-Zhi Guo:** Project administration. **Jing-Zhi Leng:** Project administration, Methodology. **Zhi-De Liang:** Supervision, Conceptualization. **Jing-Tai Wang:** Investigation, Formal analysis. **Li-Jie Luo:** Resources. **Shi-Qiang Wang:** Resources. **Yang Yuan:** Writing – review & editing, Funding acquisition.

Declaration of competing interest

The authors declare that they have no known competing financial interests or personal relationships that could have appeared to influence the work reported in this paper.

Acknowledgments

Chuanzhi Wang served as the main author and was primarily responsible for manuscript writing. Hengzhi Guo, Jingtai Wang, and Jingzhi Leng participated in the experiments. Zhide Liang contributed to the data collection, while Lijie Luo provided the research equipment. Shiqiang Wang and Yang Yuan contributed to the revision and final approval of the manuscript. All authors have contributed to the manuscript and approved the submitted version.

Appendix A. Supplementary data

Supplementary data to this article can be found online at https://doi.org/10.1016/j.heliyon.2024.e27035.

References

[1] E. Christidi, L.R. Brunham, Regulated cell death pathways in doxorubicin-induced cardiotoxicity, Cell Death Dis. 12 (4) (2021) 339.
[2] N. Wenningmann, M. Knapp, A. Ande, T.R. Vaidya, S. Ait-Oudhia, Insights into doxorubicin-induced cardiotoxicity: molecular mechanisms, preventive strategies, and early monitoring, Mol. Pharmacol. 96 (2) (2019) 219–232.
[3] O.J. Arola, A. Saraste, K. Pulkki, M. Kallajoki, M. Parvinen, L.M. Voipio-Pulkki, Acute doxorubicin cardiotoxicity involves cardiomyocyte apoptosis, Cancer Res. 60 (7) (2000) 1789–1792.
[4] S. Nagata, Apoptosis and clearance of apoptotic cells, Annu. Rev. Immunol. 36 (2018) 489–517.
[5] D.H.J. Thijssen, A. Redington, K.P. George, M.T.E. Hopman, H. Jones, Association of exercise preconditioning with immediate cardioprotection: a review, JAMA cardiology 3 (2) (2018) 169–176.
[6] I. Marques-Aleixo, E. Santos-Alves, P.J. Oliveira, P.I. Moreira, J. Magalhães, A. Ascensão, The beneficial role of exercise in mitigating doxorubicin-induced Mitochondrionopathy, Biochim. Biophys. Acta Rev. Canc 1869 (2) (2018) 189–199.
[7] S.D. Reich, F. Steinberg, N.R. Bachur, C.E. Riggs Jr., R. Goebel, M. Berman, Mathematical model for adriamycin (doxorubicin) pharmacokinetics, Cancer Chemother. Pharmacol. 3 (2) (1979) 125–131.
[8] C.Z. Wang, W. Wang, S.S. Zhang, Z.D. Liang, Y. Yuan, [Exercise preconditioning reduces exercise-induced risks of cardiovascular events in obese population], Sheng Li Xue Bao : Acta Physiol. Sin. 74 (5) (2022) 792–804.
[9] C.Y. Lien, B.T. Jensen, D.S. Hydock, R. Hayward, Short-term exercise training attenuates acute doxorubicin cardiotoxicity, J. Physiol. Biochem. 71 (4) (2015) 669–678.
[10] Y. Yuan, S.S. Pan, Y.J. Shen, Cardioprotection of exercise preconditioning involving heat shock protein 70 and concurrent autophagy: a potential chaperone-assisted selective macroautophagy effect, J. Physiol. Sci. : JPS. 68 (1) (2018) 55–67.
[11] T. Moroishi, ANXious for YAP, Nat. Chem. Biol. 17 (7) (2021) 750–751.
[12] R.H. Tao, M. Kobayashi, Y. Yang, E.S. Kleinerman, Exercise inhibits doxorubicin-induced damage to cardiac vessels and activation of hippo/YAP-mediated apoptosis, Cancers 13 (11) (2021).
[13] W.T. Chang, J.Y. Shih, Y.W. Lin, Z.C. Chen, W.C. Kan, T.H. Lin, et al., Dapagliflozin protects against doxorubicin-induced cardiotoxicity by restoring STAT3, Arch. Toxicol. 96 (7) (2022) 2021–2032.
[14] J. Zhang, Z. Sun, N. Lin, W. Lu, X. Huang, J. Weng, et al., Fucoidan from Fucus vesiculosus attenuates doxorubicin-induced acute cardiotoxicity by regulating JAK2/STAT3-mediated apoptosis and autophagy, Biomedicine & pharmacotherapy = Biomedecine & pharmacotherapie 130 (2020) 110534.
[15] J.Y. Kim, H.H. Jung, S. Ahn, S. Bae, S.K. Lee, S.W. Kim, et al., The relationship between nuclear factor (NF)-κB family gene expression and prognosis in triple-negative breast cancer (TNBC) patients receiving adjuvant doxorubicin treatment, Sci. Rep. 6 (2016) 31804.

[16] Y. Yuan, S.-S. Pan, D.-F. Wan, J. Lu, Y. Huang, H_2O_2 signaling-triggered PI3K mediates mitochondrial protection to participate in early cardioprotection by exercise preconditioning, Oxid. Med. Cell. Longev. 2018 (2018) 1916841.
[17] A.A. Kirkham, R.E. Shave, K.A. Bland, J.M. Bovard, N.D. Eves, K.A. Gelmon, et al., Protective effects of acute exercise prior to doxorubicin on cardiac function of breast cancer patients: a proof-of-concept RCT, Int. J. Cardiol. 245 (2017) 263–270.
[18] Y. Cao, Y. Ruan, T. Shen, X. Huang, M. Li, W. Yu, et al., Astragalus polysaccharide suppresses doxorubicin-induced cardiotoxicity by regulating the PI3k/Akt and p38MAPK pathways, Oxid. Med. Cell. Longev. 2014 (2014) 674219.
[19] H-g Fa, W-g Chang, X-j Zhang, D-d Xiao, J-x Wang, Noncoding RNAs in doxorubicin-induced cardiotoxicity and their potential as biomarkers and therapeutic targets, Acta Pharmacol. Sin. 42 (4) (2021) 499–507.
[20] H. Chen, C. Chen, M. Spanos, G. Li, R. Lu, Y. Bei, et al., Exercise training maintains cardiovascular health: signaling pathways involved and potential therapeutics, Signal Transduct. Targeted Ther. 7 (1) (2022) 306.
[21] S.A. Kouzi, M.N. Uddin, Aerobic exercise training as a potential cardioprotective strategy to attenuate doxorubicin-induced cardiotoxicity. Journal of pharmacy & pharmaceutical sciences : a publication of the Canadian society for pharmaceutical sciences, Societe canadienne des sciences pharmaceutiques 19 (3) (2016) 399–410.
[22] R. Domenech, P. Macho, H. Schwarze, G. Sánchez, Exercise induces early and late myocardial preconditioning in dogs, Cardiovasc. Res. 55 (3) (2002) 561–566.
[23] L. Zou, B. Liang, Y. Gao, T. Ye, M. Li, Y. Zhang, et al., Nicotinic acid riboside regulates nrf-2/P62-related oxidative stress and autophagy to attenuate doxorubicin-induced cardiomyocyte injury, BioMed Res. Int. 2022 (2022) 6293329.
[24] G.M. Stewart, A. Yamada, L.J. Haseler, J.J. Kavanagh, J. Chan, G. Koerbin, et al., Influence of exercise intensity and duration on functional and biochemical perturbations in the human heart, J. Physiol. 594 (11) (2016) 3031–3044.
[25] K.B. Wallace, V.A. Sardão, P.J. Oliveira, Mitochondrial determinants of doxorubicin-induced cardiomyopathy, Circ. Res. 126 (7) (2020) 926–941.
[26] D. Averill-Bates, A. Glory, A. Bettaieb, 281 - ROS cause pro-apoptotic changes in bcl-2 family proteins during heat shock, Free Radic. Biol. Med. 76 (2014) S120–S121.
[27] M. Zhang, J. Zheng, R. Nussinov, B. Ma, Release of cytochrome C from Bax pores at the mitochondrial membrane, Sci. Rep. 7 (1) (2017) 2635.
[28] E. Eldering, W.J. Mackus, I.A. Derks, L.M. Evers, E. Beuling, P. Teeling, et al., Apoptosis via the B cell antigen receptor requires Bax translocation and involves mitochondrial depolarization, cytochrome C release, and caspase-9 activation, Eur. J. Immunol. 34 (7) (2004) 1950–1960.
[29] W. Liao, Z. Rao, L. Wu, Y. Chen, C. Li, Cariporide attenuates doxorubicin-induced cardiotoxicity in rats by inhibiting oxidative stress, inflammation and apoptosis partly through regulation of akt/GSK-3β and Sirt1 signaling pathway, Front. Pharmacol. 13 (2022) 850053.
[30] C. Zgheib, F.A. Zouein, M. Kurdi, G.W. Booz, Differential STAT3 signaling in the heart: impact of concurrent signals and oxidative stress, JAK-STAT 1 (2) (2012) 101–110.
[31] W.-T. Chang, J.-Y. Shih, Y.-W. Lin, Z.-C. Chen, W.-C. Kan, T.-H. Lin, et al., Dapagliflozin protects against doxorubicin-induced cardiotoxicity by restoring STAT3, Arch. Toxicol. 96 (7) (2022) 2021–2032.
[32] I.M. Moya, G. Halder, Hippo-YAP/TAZ signalling in organ regeneration and regenerative medicine, Nat. Rev. Mol. Cell Biol. 20 (4) (2019) 211–226.
[33] R. Hattori, N. Maulik, H. Otani, L. Zhu, G. Cordis, R.M. Engelman, et al., Role of STAT3 in ischemic preconditioning, J. Mol. Cell. Cardiol. 33 (11) (2001) 1929–1936.
[34] L. He, H. Pratt, M. Gao, F. Wei, Z. Weng, K. Struhl, YAP and TAZ are transcriptional co-activators of AP-1 proteins and STAT3 during breast cellular transformation, Elife 10 (2021) e67312.
[35] G. Garoffolo, M. Casaburo, F. Amadeo, M. Salvi, G. Bernava, L. Piacentini, et al., Reduction of cardiac fibrosis by interference with YAP-dependent transactivation, Circ. Res. 131 (3) (2022) 239–257.